WHITEHOUSE, C. R. & BALCHIN, A. A. (1979). *J. Cryst. Growth*, **47**, 203–212.
WIEDEMEYER, H. & VON SCHNERING, H. G. (1978). *Z. Kristallogr.* **148**, 295–303.
YEOMANS, J. M. & PRICE, G. D. (1986). *Bull. Mineral.* **109**, 3–13.
ZUCKER, U. H., PERENTHALER, E., KUHS, W. F., BACHMANN, R. & SCHULZ, H. (1983). *J. Appl. Cryst.* **16**, 11–16.

Acta Cryst. (1990). **B46**, 455–458

Comparative Investigation of Microarea Quasilattice Parameters of Al–Si–Mn and Al–Cu–Fe Icosahedral Phases using HOLZ Line Patterns*

BY MINGXING DAI AND RENHUI WANG

Department of Physics, Wuhan University, 430072 *Wuhan, People's Republic of China, and Beijing Laboratory of Electron Microscopy, Academia Sinica, PO Box* 2724, 100080 *Beijing, People's Republic of China*

(*Received* 30 *October* 1989; *accepted* 1 *February* 1990)

Abstract

Some differences between the higher-order Laue zone (HOLZ) line patterns of $Al_{76}Si_4Mn_{20}$ and $Al_{65}Cu_{20}Fe_{15}$ icosahedral phases (*I* phases) have been observed. These differences originate from the fact that $Al_{76}Si_4Mn_{20}$ belongs to a simple icosahedral quasilattice whereas $Al_{65}Cu_{20}Fe_{15}$ belongs to an ordered face-centred icosahedral quasilattice, and from the minor difference in their quasilattice parameters. By computer simulation of these HOLZ line patterns using a 'standard' quasilattice parameter of 0·460 nm for the *I* phase of $Al_{76}Si_4Mn_{20}$, the quasilattice parameter of the *I* phase of $Al_{65}Cu_{20}Fe_{15}$ has been determined to be 0·8966 nm.

1. Introduction

Owing to the sensitivity of higher-order Laue zone (HOLZ) line patterns in convergent-beam electron diffraction (CBED) patterns to changes in lattice parameters (and thus to changes in the wavelength), HOLZ line patterns have been used to accurately measure the microarea lattice parameters in crystals [see, for example, Jones, Rackham & Steeds (1977), Ecob, Shaw, Porter & Ralph (1981) and Wang, Zou & Jiao (1986)]. We have recently obtained experimental HOLZ line patterns of an $Al_{76}Si_4Mn_{20}$ quasicrystalline icosahedral phase (*I* phase) with a large angular range by connecting a series of conventional CBED patterns and performing a theoretical simulation (Dai & Wang, 1990). The agreement between the experimental and theoretical HOLZ line patterns of the *I* phase has encouraged us to use HOLZ line patterns to measure the quasilattice parameter of the *I* phase accurately.

Tsai, Inoue & Masumoto (1987) reported a stable *I* phase, the $Al_{65}Cu_{20}Fe_{15}$ phase. Its composition, as determined by energy-dispersive X-ray spectrometric quantitative analysis, is $Al_{63}Cu_{24}Fe_{13}$ (Shindo, Hiraga, Williams, Hirabayashi, Inoue & Masumoto, 1989). Ebalard & Spaepen (1989) have recently studied the structure of the *I* phase of $Al_{65}Cu_{20}Fe_{15}$ by selected-area electron diffraction. They found that there are extra diffraction spots along the fivefold directions and explained this by ascribing a face-centred icosahedral (f.c.i.) structure to the *I* phase of $Al_{65}Cu_{20}Fe_{15}$, in contrast to the simple icosahedral (s.i.) structures of the *I* phases of Al_4Mn and $Al_{76}Si_4Mn_{20}$. They described the f.c.i. *I* phase of $Al_{65}Cu_{20}Fe_{15}$ as a superlattice of the s.i. lattice by placing two kinds of atomic clusters at even and odd vertices (ordering). Moreover, we expect there would be a minor difference between the quasilattice parameters of the *I* phases of $Al_{76}Si_4Mn_{20}$ and $Al_{65}Cu_{20}Fe_{15}$ owing to differences in both the chemical composition and the ordering.

The purpose of the present work is to observe whether there are extra HOLZ lines in the *I* phase of $Al_{65}Cu_{20}Fe_{15}$ caused by superreflections, and to determine the quasilattice parameter of this phase for comparison with that of the *I* phase of $Al_{76}Si_4Mn_{20}$.

2. Experimental and simulation

The rapidly solidified ternary $Al_{76}Si_4Mn_{20}$ and $Al_{65}Cu_{20}Fe_{15}$ ribbons were obtained from prealloyed ingots by the melt-spinning method. Specimens for transmission electron microscopy were then prepared by ion milling and observed with a Philips EM420 electron microscope operated at an accelerating voltage of 100 kV. The CBED patterns were photographed at liquid-nitrogen temperature using a low-temperature double-tilting stage.

* Project supported by the National Natural Science Foundation of China.

0108-7681/90/040455-04$03.00

The HOLZ line pattern of the s.i. *I* phase of $Al_{76}Si_4Mn_{20}$ was simulated according to Dai & Wang (1990) with a quasilattice parameter $a_0 = 0{\cdot}460$ nm, as reported by Elser (1985). Because the electron diffraction patterns of the $Al_{65}Cu_{20}Fe_{15}$ *I* phase were explained in terms of an f.c.i. quasilattice caused by ordering (Ebalard & Spaepen, 1989), we choose its quasilattice parameter a_f to be nearly $2a_0$. Therefore, a diffraction spot with indices n_1^*, n_2^*, n_3^*, n_4^*, n_5^*, n_6^* for s.i. $Al_{76}Si_4Mn_{20}$ should be indexed as $2n_1^*$, $2n_2^*$, $2n_3^*$, $2n_4^*$, $2n_5^*$, $2n_6^*$ for f.c.i. $Al_{65}Cu_{20}Fe_{15}$ and there are some superreflections for f.c.i. $Al_{65}Cu_{20}Fe_{15}$ with all-odd indices.

3. Results

Fig. 1(*a*) shows the simulated HOLZ line pattern obtained by connecting seven patterns covering the whole orientation triangle of the $Al_{76}Si_4Mn_{20}$ *I* phase (Dai & Wang, 1990). The circled region in Fig. 1(*a*) is enlarged and shown in Fig. 1(*b*) with more HOLZ lines. Figs. 2(*a*) and 2(*b*) show the experimental HOLZ line patterns for s.i. $Al_{76}Si_4Mn_{20}$ and f.c.i. $Al_{65}Cu_{20}Fe_{15}$, respectively. The orientation of these patterns is circled in Fig. 1(*b*). During the process of computer simulation, we fixed the quasilattice parameter of s.i. $Al_{76}Si_4Mn_{20}$ at $a_0 = 0{\cdot}460$ nm and changed the effective wavelength to arrive at the agreement between the experimental HOLZ line pattern (Fig. 2*a*) and the simulated one. Then, by using the effective wavelength value ($\lambda = 0{\cdot}00369$ nm) and changing the quasilattice parameter a_f, we arrived at the best agreement between the experimental and simulated HOLZ line patterns for f.c.i. $Al_{65}Cu_{20}Fe_{15}$ when $a_f = 0{\cdot}8966$ nm. Figs. 3(*a*) and 3(*b*) are computer-simulated HOLZ line patterns corresponding to Figs. 2(*a*) and 2(*b*), and with quasilattice parameters $a_0 = 0{\cdot}460$ nm and $a_f = 0{\cdot}8966$ nm, respectively. The reflection indices n_1^*, n_2^*, n_3^*, n_4^*, n_5^*, n_6^* of the HOLZ lines are listed in Table 1 for both s.i. $Al_{76}Si_4Mn_{20}$ and f.c.i. $Al_{65}Cu_{20}Fe_{15}$ quasicrystals.

By comparing the CBED patterns of the s.i. $Al_{76}Si_4Mn_{20}$ (Fig. 2*a*) and f.c.i. $Al_{65}Cu_{20}Fe_{15}$ (Fig. 2*b*) quasicrystals, it is found that their main features are similar with only some minor differences. Firstly, HOLZ line 8 in Fig. 2(*b*) with all-odd indices (see Table 1) does not exist in Fig. 2(*a*) (arrowed). This can be explained if line 8 corresponds to a superreflection caused by ordering in the *I* phase of $Al_{65}Cu_{20}Fe_{15}$. There are further superreflections in the CBED pattern of the f.c.i. $Al_{65}Cu_{20}Fe_{15}$ specimen which do not appear in s.i. $Al_{76}Si_4Mn_{20}$. Nonetheless, their corresponding HOLZ lines cannot be seen in Fig. 2(*b*) because the intensities of these superreflections are too weak. Secondly, three HOLZ lines (1, 4 and 7) intersect with each other almost at a point in Fig. 2(*a*) but form a small triangle in Fig. 2(*b*). Moreover, the ratios of the two line segments (*AB* and *BC*) are different in Figs. 2(*a*) and 2(*b*). Such differences in the geometrical features of the HOLZ line patterns are caused by differences in the quasilattice parameters and this is the reason why we can accurately measure differences in the quasilattice parameters using HOLZ line patterns and their simulations.

4. Discussion

The advantage of the HOLZ line method for measuring the lattice or quasilattice parameters lies in the fact that the parameter of a microarea with a diameter of some nanometers can be measured with a small error (less than one thousandth). In the present work a one-thousandth variation in the value of the

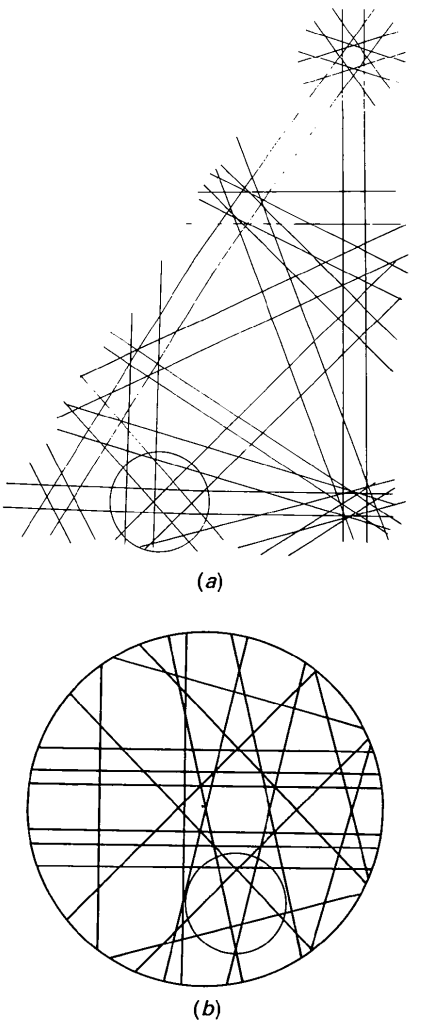

Fig. 1. (*a*) Simulated HOLZ line pattern of an s.i. $Al_{76}Si_4Mn_{20}$ quasicrystal covering the whole orientation triangle. (*b*) Detail of the circled area in (*a*) showing the orientation of experimental HOLZ line patterns in the present work.

wavelength or quasilattice parameter may cause a discernible change in the HOLZ line pattern. If orientations with higher sensitivity to changes of the HOLZ line pattern are found, better measuring accuracy may be attained. The absolute accuracy of the measured quasilattice parameter is limited by the accuracy of the value of the wavelength and the dynamical diffraction effect (Jones *et al.*, 1977) because we have simulated HOLZ line patterns using the kinematical diffraction approximation. In this work an $Al_{76}Si_4Mn_{20}$ quasicrystalline specimen with a quasilattice parameter $a_0 = 0{\cdot}460$ nm (Elser, 1985) was used as the standard to determine the wavelength. Because the *I* phases of both $Al_{76}Si_4Mn_{20}$ and of $Al_{65}Cu_{20}Fe_{15}$ (or $Al_{63}Cu_{24}Fe_{13}$) consist of Mackay icosahedra and their differences in chemical composition and atomic structure have only secondary effects the error in the kinematically simulated HOLZ line patterns for these two specimens caused by the dynamical diffraction effect should be compensated for. The value $a_0 = 0{\cdot}460$ nm for s.i. $Al_{76}Si_4Mn_{20}$ was obtained by Elser (1985) from the experimental values of the reciprocal vector determined by high-resolution X-ray powder diffraction (Bancel, Heiney, Stephens, Goldman & Horn, 1985). The accuracy of this value is believed to be about one thousandth. As mentioned above, the sensitivity of the HOLZ line pattern in the present work is about one thousandth. Therefore, the quasilattice parameter, $a_f = 0{\cdot}8966$ nm, measured in the present work has an absolute accuracy of about one thousandth.

A comparison of the experimental a_f values of f.c.i. $Al_{65}Cu_{20}Fe_{15}$ is given in Table 2. The table lists the quasilattice parameters corresponding to the indexing system used by Elser (1985) for s.i. $Al_{76}Si_4Mn_{20}$ ($a_0 = 0{\cdot}4597$ nm) and by us for f.c.i. $Al_{65}Cu_{20}Fe_{15}$. The indexing systems of Tsai *et al.* (1987) and Ebalard *et al.* (1989) are different from those of the present work by the deflation and

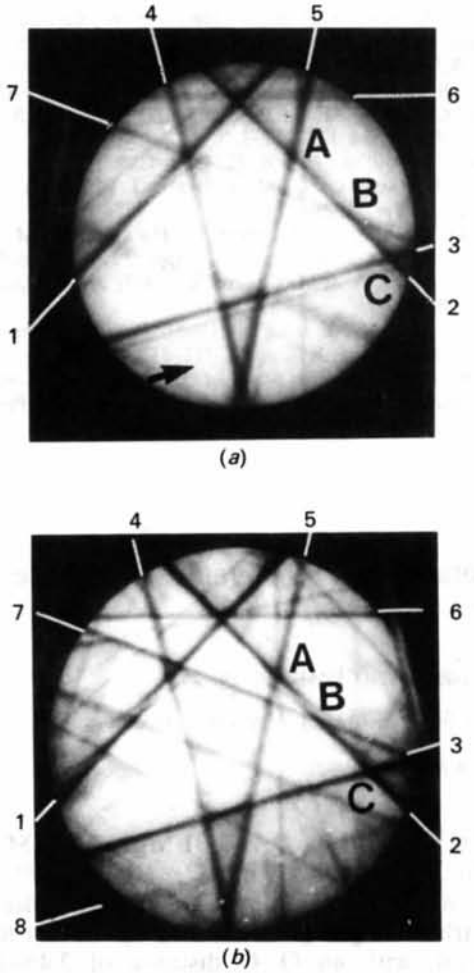

Fig. 2. Experimental HOLZ line patterns for (*a*) s.i. $Al_{76}Si_4Mn_{20}$ and (*b*) f.c.i. $Al_{65}Cu_{20}Fe_{15}$ quasicrystals.

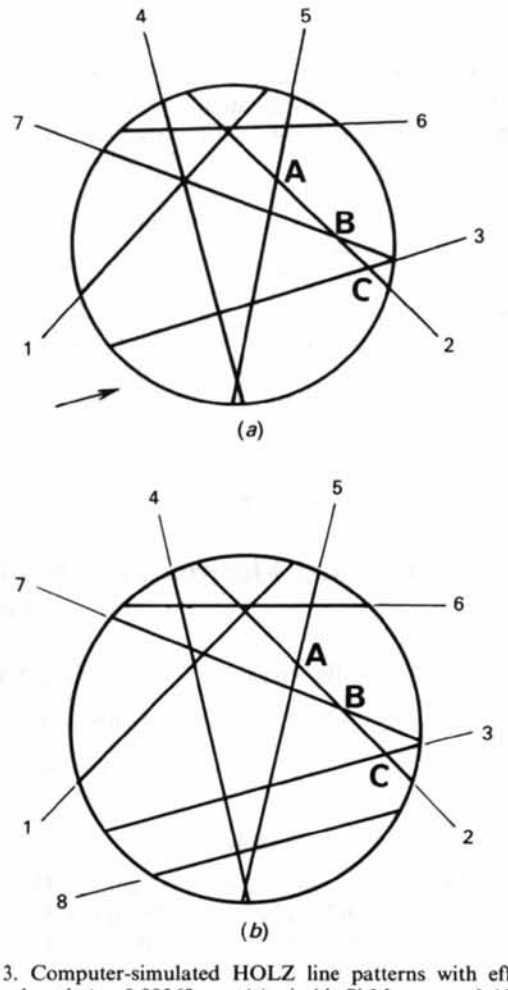

Fig. 3. Computer-simulated HOLZ line patterns with effective wavelength $\lambda = 0{\cdot}00369$ nm: (*a*) s.i. $Al_{76}Si_4Mn_{20}$, $a_0 = 0{\cdot}460$ nm; (*b*) f.c.i. $Al_{65}Cu_{20}Fe_{15}$, $a_f = 0{\cdot}8966$ nm.

Table 1. *Indices and the calculated moduli of the reciprocal vector* **g** *and Bragg angles* θ *of HOLZ lines shown in Figs. 2 and 3*

	s.i. Al–Mn–Si								f.c.i. Al–Cu–Fe							
Line No.	n_1^*	n_2^*	n_3^*	n_4^*	n_5^*	n_6^*	g	θ (°)	n_1^*	n_2^*	n_3^*	n_4^*	n_5^*	n_6^*	g	θ (°)
1	−1	−1	−4	−2	2	3	0·9086	0·9610	−2	−2	−8	−4	4	6	0·9323	0·9861
2	−2	−4	−1	2	1	−3	0·9086	0·9610	−4	−8	−2	4	2	−6	0·9323	0·9861
3	2	3	4	1	−2	−1	0·9086	0·9610	4	6	8	2	−4	−2	0·9323	0·9861
4	−1	−2	1	2	0	−3	0·6681	0·7066	−2	−4	2	4	0	−6	0·6855	0·7251
5	0	1	−2	−2	1	3	0·6681	0·7066	0	2	−4	−4	2	6	0·6855	0·7251
6	−3	−5	−5	0	3	0	1·2675	1·3405	−6	−10	−10	0	6	0	1·3005	1·3755
7	3	5	3	−1	−2	2	1·1078	1·1717	6	10	6	−2	−4	4	1·1367	1·2022
8									3	3	5	1	−3	−1	0·6572	0·6950

Table 2. *Comparison of the measured values of the quasilattice parameters*

	s.i. $Al_{76}Si_4Mn_{20}$	f.c.i. $Al_{65}Cu_{20}Fe_{15}$		
	Elser (1985) and Bancel *et al.* (1985)	Tsai *et al.* (1987)	Ebalard & Spaepen (1989)	This work
Indices	211111	100000	1888888	422222
$2\pi g$ (nm^{-1})	28·96	29·76	29·8	
a (nm)	0·4595	$0{\cdot}894_2$	$0{\cdot}893_2$	
Indices	221001	110000	1610001016	442002
$2\pi g$ (nm^{-1})	30·43	31·41	31·3	
a (nm)	0·4598	$0{\cdot}891_0$	$0{\cdot}894_1$	
Averaged a (nm)	0·4597	$0{\cdot}892_6$	$0{\cdot}893_6$	$0{\cdot}896_6$

inflation factors of $\tau^{-3}/2$ and τ^3, respectively, with $\tau = (\sqrt{5}+1)/2$ the golden mean. When quasilattice parameters for f.c.i. $Al_{65}Cu_{20}Fe_{15}$ are reduced to the s.i. lattice (divided by a factor of two) they become about 2·5% smaller than those of s.i. $Al_{76}Si_4Mn_{20}$. Noticing that the values of the atomic radii are 1·43, 1·17, 1·12, 1·28 and 1·28 Å for Al, Si, Mn, Cu and Fe, respectively (Wood, 1971), the mean atomic radii for $Al_{76}Si_4Mn_{20}$, $Al_{65}Cu_{20}Fe_{15}$ and $Al_{63}Cu_{24}Fe_{13}$ are 1·36, 1·38 and 1·37 Å, respectively. Therefore, this difference of 2·5% cannot be explained by the difference in the mean atomic radii. A possible explanation may be an ordering effect which may induce a shrinkage of the quasilattice.

We would like to thank Professor F. H. Li, Dr M. J. Hui and Dr Y. F. Cheng of the Institute of Physics, Academia Sinica, for providing the specimen of $Al_{65}Cu_{20}Fe_{15}$ and for sending us their unpublished research report.

References

BANCEL, P. A., HEINEY, P. A., STEPHENS, P. W., GOLDMAN, A. I. & HORN, P. M. (1985). *Phys. Rev. Lett.* **54**, 2422–2425.

DAI, M. & WANG, R. (1990). *Solid State Commun.* **73**, 77–80.

EBALARD, S. & SPAEPEN, F. (1989). *J. Mater. Res.* **4**, 39–43.

ECOB, R. C., SHAW, M. P., PORTER, A. J. & RALPH, B. (1981). *Philos. Mag. A*, **44**, 1117–1133.

ELSER, V. (1985). *Phys. Rev. B*, **32**, 4892–4898.

JONES, P. M., RACKHAM, G. M. & STEEDS, J. W. (1977). *Proc. R. Soc. London Ser. A*, **354**, 197–222.

SHINDO, D., HIRAGA, K., WILLIAMS, T., HIRABAYASHI, M., INOUE, A. & MASUMOTO, T. (1989). *Jpn. J. Appl. Phys.* **28**, L688–L689.

TSAI, A. P., INOUE, A. & MASUMOTO, T. (1987). *Jpn. J. Appl. Phys.* **26**, L1505–L1507.

WANG, R., ZOU, H. & JIAO, S. (1986). *Proc. 11th Int. Congr. Electron Microscopy*, Kyoto, pp. 711–712.

WOOD, W. A. (1971). *The Study of Metal Structures and Their Mechanical Properties*, p. 369. New York: Pergamon Press.

Acta Cryst. (1990). B**46**, 458–466

Structure and Electron Density of Nickel Potassium Hydrogenbiscarbonate Tetrahydrate

BY NELSON G. FERNANDES,* ROLAND TELLGREN AND IVAR OLOVSSON

Institute of Chemistry, University of Uppsala, Box 531, S-751 21 Uppsala, Sweden

(*Received* 4 *December* 1989; *accepted* 14 *February* 1990)

Abstract

$KNiH(CO_3)_2.4H_2O$, $M_r = 290{\cdot}7$, triclinic, $P\bar{1}$, $a = 5{\cdot}3824\ (2)$, $b = 6{\cdot}6737\ (2)$, $c = 6{\cdot}9480\ (2)$ Å, $\alpha = 115{\cdot}881\ (2)$, $\beta = 90{\cdot}678\ (2)$, $\gamma = 108{\cdot}017\ (2)°$, $V = 210{\cdot}37\ (1)$ Å^3, $Z = 1$, $D_x = 2{\cdot}31$ Mg m^{-3}, λ(Mo $K\alpha$) $= 0{\cdot}71073$ Å, $\mu = 2{\cdot}859$ mm^{-1}, $F(000) = 148$, $T = 298$ K, $R(F^2) = 0{\cdot}0350$ for 5228 unique reflections. Two carbonate groups are linked by a short hydrogen bond, with an O···O distance of 2·456 (2) Å, forming a nearly planar centrosymmetric anion, $[H(CO_3)_2]^{3-}$. The non-spherical distribution of the

* Permanent address: Department of Chemistry, Federal University of Minas Gerais, CP 702, 30161 Belo Horizonte, Brazil.

0108-7681/90/040458-09$03.00